Atherosclerotic cardiovascular disease: interplay between sex, age, and circadian rhythms

In het Panhuis, W.

7

Time-restricted feeding attenuates hyper-cholesterolemia and atherosclerosis development during circadian disturbance in APOE*3-Leiden.CETP mice

Wietse In het Panhuis[1,2], Milena Schönke[1,2], Melanie Modder[1,2], Hannah E. Tom[1,2], Reshma A. Lalai[1,2], Amanda C.M. Pronk[1,2], Trea C.M. Streefland[1,2], Linda W.M. van Kerkhof[3], Martijn E.T. Dollé[3], Marie A.C. Depuydt[4], Ilze Bot[4], Winnie G. Vos[5,6,7], Laura A. Bosmans[5,6,7], Bram W. van Os[5,6,7], Esther Lutgens[5,6,7,8], Patrick C.N. Rensen[1,2], and Sander Kooijman[1,2]

[1]Division of Endocrinology, Department of Medicine, Leiden University Medical Center, Leiden, The Netherlands
[2]Einthoven Laboratory for Experimental Vascular Medicine, Leiden University Medical Center, Leiden, The Netherlands.
[3]Centre for Health Protection, National Institute for Public Health and the Environment, Bilthoven, The Netherlands
[4]Leiden Academic Centre for Drug Research, Division of Biotherapeutics, Leiden University, Leiden, the Netherlands
[5]Amsterdam UMC location University of Amsterdam, Department of Medical Biochemistry, Amsterdam, the Netherlands
[6]Amsterdam Cardiovascular Sciences, Atherosclerosis & Ischemic Syndromes, Amsterdam, the Netherlands
[7]Amsterdam Immunity and Infection, Amsterdam, the Netherlands
[8]Department of Cardiovascular Medicine, Mayo Clinic, Rochester, Minnesota, USA

eBioMedicine, in revision

Abstract

Circadian disturbance (CD) is the consequence of a mismatch between endogenous circadian rhythms, behavior, and/or environmental cycles, and frequently occurs during shift work. Shift work has been associated with elevated risk for atherosclerotic cardiovascular disease (asCVD) in humans, but evidence for the effectiveness of prevention strategies are lacking. Here, we applied time-restricted feeding (TRF) as a strategy to counteract atherosclerosis development during CD in female APOE*3-Leiden.CETP mice, a well-established model for humanized lipoprotein metabolism. Control groups were subjected to a fixed 12:12 hour light-dark cycle, while CD groups were subjected to a 6-hour phase advancement every 3 days. Groups had either *ad libitum* (AL) access to food or were subjected to TRF with restricted food access to the dark phase. TRF did not prevent the increase in the relative abundance of circulating inflammatory monocytes and elevation of (postprandial) plasma triglycerides during CD. Nonetheless, TRF reduced atherosclerotic lesion size and prevented elevated macrophage content of atherosclerotic lesions during CD, while increasing relative abundance of anti-inflammatory monocytes, preventing activation of T cells, and lowering plasma total cholesterol levels and markers of hepatic cholesterol synthesis. These effects were independent of total food intake. We propose that time restricted eating could be a promising strategy for the primary prevention of asCVD risk in shift workers, which warrants future study in humans.

Introduction

Cardiovascular diseases (CVDs) are the leading cause of mortality with approximately 30% of global deaths attributed to cardiovascular events.[1] The main pathology underlying CVD is atherosclerosis, which is the result of progressive accumulation of lipids and immune cells and chronic low-grade inflammation in arteries. Current strategies to treat atherosclerotic (as)CVD focus on traditional risk factors, such as hypertension and dyslipidemia. Despite their effectiveness, a considerable residual risk remains that may be attributed to non-traditional risk factors, including circadian disturbance (CD) that is caused by misalignment between circadian rhythms.[2]

Circadian rhythms are generated by a transcription-translation feedback loop, which is present in all cells of the body and under control of the suprachiasmatic nucleus (SCN). The SCN receives information about environmental light, and light thereby finetunes rhythms and allows for alignment of these rhythms with and adaptation to seasonal changes in environmental light-dark cycles. Light is accordingly referred to as the main *Zeitgeber*. This way, the circadian system regulates, for example, energy metabolism in a time of day-dependent manner in anticipation of daily variation in nutrient availability and requirements. However, modern society behavior does often not align with physiological circadian rhythms, resulting in CD, which has been associated with increased risk for cardiometabolic diseases in humans.[3-8] We previously demonstrated that CD is causally linked to accelerated atherosclerosis development in APOE*3-Leiden.CETP mice,[9] a well-established humanized mouse model for lipoprotein metabolism and atherosclerosis development.[10,11] Given the increasing prevalence of severe CD as a result of large-scale shift work, effective forms of primary prevention to minimize the consequences of CD on asCVD risk are highly warranted.

A potential non-pharmacological approach to prevent cardiovascular problems associated with CD is time-restricted eating (TRE), which is an emerging paradigm that restricts food intake to a pre-defined shortened daily time-window and is referred to as time-restricted feeding (TRF) when applied in animal studies. In humans, TRE promotes weight loss and improves cardiometabolic health irrespective of ethnicity.[12,13] In mice, TRF has additionally been shown to dictate diurnal gene expression patterns of peripheral tissues, such as the liver independently of light-dark cycles, demonstrating that food intake also acts as a *Zeitgeber*.[12,14] In addition, we previously demonstrated that TRF can accelerate adaptation to changes in the light-dark cycle.[15] Based on these data, we hypothesized that TRF can aid in the protection from cardiometabolic disorders caused by CD. In the current study, we demonstrate that TRF attenuates the development of hypercholesterolemia and atherosclerosis in APOE*3-Leiden.CETP mice subjected to CD.

Materials and methods

Animals

Female APOE*3-Leiden.CETP mice were used, as they develop hypercholesterolemia and atherosclerosis when fed a cholesterol-rich Western-type diet,[10,16] and were generated as previously described.[11] Mice were housed in groups of 2-3 animals per cage in cabinets equipped with diffuse white fluorescent light (550-600 lux; Bailey True-Light fluorescent tubes, 139985, Technische Unie, Alphen aan de Rijn, The Netherlands) at 21°C. Five weeks prior to the start of the intervention, the mice (7-15 weeks of age) were switched to Western-type diet containing 16% fat and 0.10% cholesterol (Diet T; Ssniff-Spezialdiäten GmbH, Soest, Germany), and mice continued to receive this diet throughout the intervention. After this adjustment period of 5 weeks, mice were randomized to one of four intervention groups (RandoMice software, Leiden, the Netherlands[17]). Control groups were subjected to a fixed 12:12 hour light-dark cycle, while CD groups were subjected to a phase advancement of 6 hours (i.e. shortening of the dark phase) every 3 days. Groups had either unrestricted (*ad libitum*, AL) access to food, or the access was restricted to the dark phase (TRF) using an automated feeding system (FeedTime, TSE-Systems GmbH, Berlin, Germany). The resulting four experimental groups (n=16 per group) were therefore defined as Control + AL, CD + AL, Control + TRF, CD + TRF. Blinding of the group assignment was not possible due to the nature of the intervention.

All measurements were conducted on the day after a shift in light-dark cycle for the CD groups, and only when the light-dark cycles of the experimental groups were aligned (occurring every 11 days after 4 consecutive phase shifts in de CD group, referred to as “cycle of phase shifts”; the total duration of the intervention was 14 weeks, or nine cycles of phase shifts), unless indicated otherwise. Body weight was monitored using a scale and body composition was determined with EchoMRI (EchoMRI 100-Analyzer; EchoMRI, Houston, Texas). Blood was collected from the tail vein at indicated time points to measure plasma lipid levels. Additional blood was collected during the third cycle of phase shifts to determine diurnal variation in plasma lipid levels relatively early on in the study to select time points for follow-up measurements. A pre-defined subset of mice (n=8 per group) was fasted for 4 hours and subjected to a lipid tolerance test starting at ZT12 during the seventh cycle of phase shifts. Abundance of circulating immune cells was determined at two time points (n=8 per group per time point) during the ninth cycle of phase shifts. After 9 cycles, mice were injected at two time points (n=8 per group per time point; time difference between the first and last mouse was approximately 2 hours) with radiolabeled triglyceride (TG)-rich lipoprotein (TRL)-mimicking particles. Mice were killed with CO_2 15 minutes after the injection, and subsequently perfused transcardially with ice-cold PBS for 5 minutes before organs were collected to assess plasma clearance and organ uptake of TRL-mimicking particles, and for other analyses. One mouse of the CD + AL group died prematurely after fighting, and three mice of the

Control + TRF and two mice of the CD + TRF group were excluded from the analysis due to technical failure of the automated feeding systems.

Voluntary physical activity and rhythm strength

Passive infrared sensors were used to measure activity of the mice within their home-cage during the second cycle of phase shifts to assess rhythms in voluntary activity early during the intervention. Passive infrared sensor data were used to generate representative actograms to construct F-periodograms using Clocklab software version 6.1.05 (Actimetrics Software, Wilmette, Illinois, USA). Rhythm strength was derived from the amplitude of corresponding periodograms.[18,19]

Indirect calorimetry

Energy expenditure was assessed in home-cages by means of indirect calorimetry (Promethion System; Sable Systems, Las Vegas, Nevada, USA) during the sixth cycle of phase shifts. Data on food intake, O_2 consumption, and CO_2 production were continuously collected in 5 minute bins, and energy expenditure was calculated. Data of two consecutive light-dark cycles was analyzed, starting directly after the phase advancement in the CD group.

Atherosclerosis quantification

Hearts were excised, fixated in 4% formaldehyde for 24 hours and stored in 70% ethanol prior to embedding in paraffin and cross-sectioning using a microtome (5 µm sections). Cross sections were stained with hematoxylin-phloxine-saffron (HPS). Atherosclerotic lesion sizes of four cross sections throughout the aortic root with a distance of 50 µm, starting at open aortic valves, were quantified with imaging software (ImageJ version 1.52a; National Institutes of Health, Bethesda, Maryland). Atherosclerotic plaques were scored subjectively for lesion severity (Mild: type I-III lesions; Severe: type IV-V lesions), according to the guidelines of the American Heart Association adapted for mice, as previously described.[10] Monoclonal mouse antibody (1:1000; M0851; Dako, Heverlee, The Netherlands) against smooth muscle cell α-actin and secondary goat anti-mouse IgG (1:400; K4003; Dako, Heverlee, The Netherlands) were used to quantify smooth muscle cells. Quantification of macrophage content was performed by staining with rat monoclonal anti-mouse MAC-3 antibody (1:1000; 550292; BD Pharmingen, San Diego, USA) and secondary goat anti-rat IgG (MP7444; Vector Laboratories Inc., Burlingame, USA). The immunoperoxidase complexes on the secondary antibodies were visualized with Liquid Dab + Substrate Chromogen System (K3468, Dako, Heverlee, The Netherlands) and Nova Red (SK-4800, Vector Laboratories Inc., Burlingame, USA) for the smooth muscle cell and macrophage quantification, respectively. A solution of direct red (365548-5G) and fast green (F7258S) (both 1:1000; Sigma Aldrich, St. Louis, USA) was used to stain collagen. Sample numbers were blinded prior to atherosclerosis quantification.

Flow cytometry

Whole blood was incubated with hypotonic lysis buffer (160 mM ammonium chloride, 10 mM sodium bicarbonate, 1.3 mM ethylenediaminetetraacetic acid (EDTA); pH 7.4) to remove erythrocytes. Samples were resuspended and stained in staining buffer (0.5% bovine serum albumin, 5 mM EDTA in PBS; pH 7.4). Myeloid populations were identified using the following antibodies: αCCR2 (1:100, BV711, #747964, BD Biosciences, Franklin Lakes, New Jersey, USA), αCD11b (1:200, PerCP-Cy5.5, #550993, BD Biosciences), αCD11c (1:100, PE-Cy7, #25-0114, Thermo Fisher Scientific, Waltham, Massachusetts, USA), αCD16/32α (1:1000, #101330, BioLegend, San Diego, California, USA), αCD40 (1:100, PE, #124609, BioLegend), αCD45 (1:200, APC-Cy7, #103115, BioLegend), αCD86 (1:100, BV650, #105035, BioLegend), αLy6C (1:800, AF647, #128010, BioLegend), αLy6G (1:200, FITC, #11-5931, Thermo Fisher Scientific), αMHCII (1:200, BV510, #107635, BioLegend), and αSiglec-F (1:100, BV421, #562681, BD Biosciences). To identify T population, samples were stained with the following antibodies: αB220 (1:200, APC-eFluor780, #47-0452, Thermo Fisher Scientific), αCCR2 (1:100, BV711, #747964, BD Biosciences), αCD3 (1:100, BV510, #100353, BioLegend), αCD4 (1:800, BV650, 100469, BioLegend), αCD8 (1:1000, BV605, #100744, BioLegend), αCD16/32α (1:1000, #101330, BioLegend), CD19 (1:200, PerCP-Cy5.5, #45-0193, Thermo Fisher Scientific), αCD40 (1:100, PE, #124609, BioLegend), αCD44 (1:300, FITC, #103006, BioLegend), αCD62L (1:1000, PE-Cy7, #104418, BioLegend), and αCXCR3 (1:200, APC, #126511, BioLegend). Prior to analysis DAPI was added (final concentration of 15 ng/mL, D21490, Thermo Fisher Scientific) to exclude dead cells. Cells were measured on a LSRFortessa Cell Analyzer (BD Biosciences) and data was analyzed using FCS Express software, version 7 (De Novo Software).

Plasma measurements

Plasma TG and total cholesterol (TC) levels were measured utilizing enzymatic Cobas Triglycerides (106571) or Cobas Total Cholesterol (106570) kits (both from Roche Diagnostics, Mannheim, Germany), by combining 7.5 µL sample (5x diluted) with 200 µL reagent (reagent was undiluted for TG and 3× diluted for TC) prior to incubation at room temperature for 30 minutes and measuring transmittance at 492 nm versus 650 nm (for TG) or at 505 nm versus 650 nm (for TC). To calculate total TC exposure, the area under the curve was determined from regularly monitored plasma TC levels over time.

Postprandial lipid tolerance

Mice received an oral olive oil bolus via gavage (8 µL/g body weight per mouse) (Carbonell, Cordoba, Spain). Tail vein blood was sampled at indicated time points to measure plasma TG levels.

Clearance of radiolabeled lipoprotein-like emulsion particles

Mice were intravenously injected with an emulsion of TG-rich lipoprotein-like particles (80 nm) that were double-labelled with glycerol tri[^{3}H]oleate and [^{14}C]cholesteryl oleate (1 mg TG in 200 µL saline per mouse), prepared as described previously.[20] Blood was

collected at indicated time points to determine plasma decay of radiolabels. Tissues (approx. 50-200 mg) were dissolved in 0.5 mL Solvable (6NE9100, PerkinElmer, Waltham, Massachusetts, USA) at 56°C overnight, after which 5.0 mL Ultima Gold (6013329, PerkinElmer, Waltham, Massachusetts, USA) was added. Plasma (4 µL) was directly added to 2.5 mL Ultima Gold. ^{3}H-and ^{14}C-activity was measured with a liquid scintillation counter (Tri-Carb 2910 TR, PerkinElmer, Waltham, Massachusetts, USA) and expressed as a percentage of injected dose per whole tissue or as a percentage of injected dose in plasma. One mouse was excluded for calculating the AUC (between 2 and 15 minutes after injection) of plasma decay since one plasma sample was missing.

Gene expression

RNA was isolated from frozen liver (approx. 30 mg) by lysis and homogenization using TriPure RNA Isolation Reagent (11667165001, Sigma-Aldrich, Saint Louis, USA) and a FastPrep-24™ 5G bead beating grinder and lysis system (4.0 m/s for 10 sec; MP Biomedicals™, Santa Ana, California, USA). cDNA was synthesized from 1 µg RNA using M-MLV Reverse Transcriptase (M1705, Promega, Madison, USA) and qPCR was conducted utilizing SYBR green kit (Promega, Madison, Wisconsin, USA) and a CFX96 PCR machine (Bio-Rad, Hercules, USA), according to the manufacturers' protocols. Gene expression was normalized to glyceraldehyde-3-phosphate dehydrogenase (*Gapdh*) and expressed relative to the Control + AL group at ZT0. Primer sequences are provided in Table 1.

Table 1. primer sequences

Gene	Forward primer	Reverse primer
Abcg5	TGTCCTACAGCGTCAGCAACC	GGCCACTCTCGATGTACAAGG
Apob	GCCCATTGTGGACAAGTTGATC	CCAGGACTTGGAGGTCTTGGA
Bmal1	ATGCCAAGACTGGACTTCCG	TGCAGAAGCTTTTTCGATCTGC
Clock	AGTTAGGGCTGAAAGACGGC	GGTGTGGAGGAAGGGTCTGA
Cyp7a1	CAGGGAGATGCTCTGTGTTCA	AGGCATACATCCCTTCCGTGA
Gapdh	GGGGCTGGCATTGCTCTCAA	TTGCTCAGTGTCCTTGCTGGGG
Hmgcr	CCGGCAACAACAAGATCTGTG	ATGTACAGGATGGCGATGCA
Mttp	CTCTTGGCAGTGCTTTTTCTCT	GAGCTTGTATAGCCGCTCATT
Per2	TGTGTGCTTACACGGGTGTCCTA	ACGTTTGGTTTGCGCATGAA
Srebp2	TGAAGCTGGCCAATCAGAAAA	ACATCACTGTCCACCAGACTGC

Ethics statement

Experiments were performed in accordance with the Institute for Laboratory Animal Research Guide for the Care and Use of Laboratory Animals, and were approved by the National Committee for Animal Experiments of the Netherlands and by the Ethics Committee on Animal Care and Experimentation of the Leiden University Medical

Center. All animal procedures were conformed the guidelines from Directive 2010/63/EU of the European Parliament on the protection of animal used for scientific purposes.

Statistical analyses

The primary outcome was atherosclerotic lesion size, of which we anticipated a 40% difference to be biologically relevant and expected a standard deviation of 33%. Therefore, 16 mice per group were needed with a power of 80%, an acceptable type I error rate of 5%, and four pair-wise comparisons. Significant outliers were identified with a Grubbs outlier test and removed from the analysis (α=5%). Statistical analyses between groups were performed with unpaired t-test, two-way or three-way analysis of variance (ANOVA) and following Tukey's multiple-comparison post-hoc test, where applicable. Pearson product-moment correlation coefficients were determined to assess linear correlations between variables. $P<0.05$ was considered statistically significant. Statistical analyses were performed with GraphPad Prism software, version 9.3.1 (GraphPad, La Jolla, California). Data are presented as individual data points and/or as means ± SD.

Results

Time-restricted feeding does not change behavior or whole-body energy balance during circadian disturbance

APOE*3-Leiden.CETP mice were subjected to a fixed 12:12 hour light-dark cycle (Control groups) or to a 6-hour light phase advancement every 3 days (CD groups). CD was confirmed through monitoring of voluntary physical activity during the second cycle of four consecutive phase shifts (Fig. 1a), and from which rhythm strength (Fig. 1b) and period (Fig. 1c) were calculated. TRF seemed to partly prevent the reduction in rhythm strength caused by CD, although rhythm strength in the CD+TRF group was not statistically different from CD+AL. We next assessed diurnal food intake and whole-body energy balance during the sixth cycle of phase shifts. Two consecutive 12:12 hour light-dark cycles were analyzed, starting directly after the phase advancement in the CD groups. CD caused a shift in food intake and energy expenditure, without altering total daily levels (Fig. 1d-g). In line with rhythm strength, TRF partly prevented the shift in energy expenditure from the dark to the light phase seen with CD, but without significant differences between the CD+TRF and CD+AL group (Fig. 1f). CD did not alter body weight and composition (Fig. 2a-c), tissue weights of liver, white adipose tissue (WAT), and brown adipose tissue (BAT) (Fig. 2d), or hepatic lipid content (Fig. 2e-g), regardless of TRF. Interestingly, TRF induced variation between ZT0 and ZT12 in hepatic lipid content when mice were exposed to normal light-dark cycles but not during CD (Fig. 2e-g).

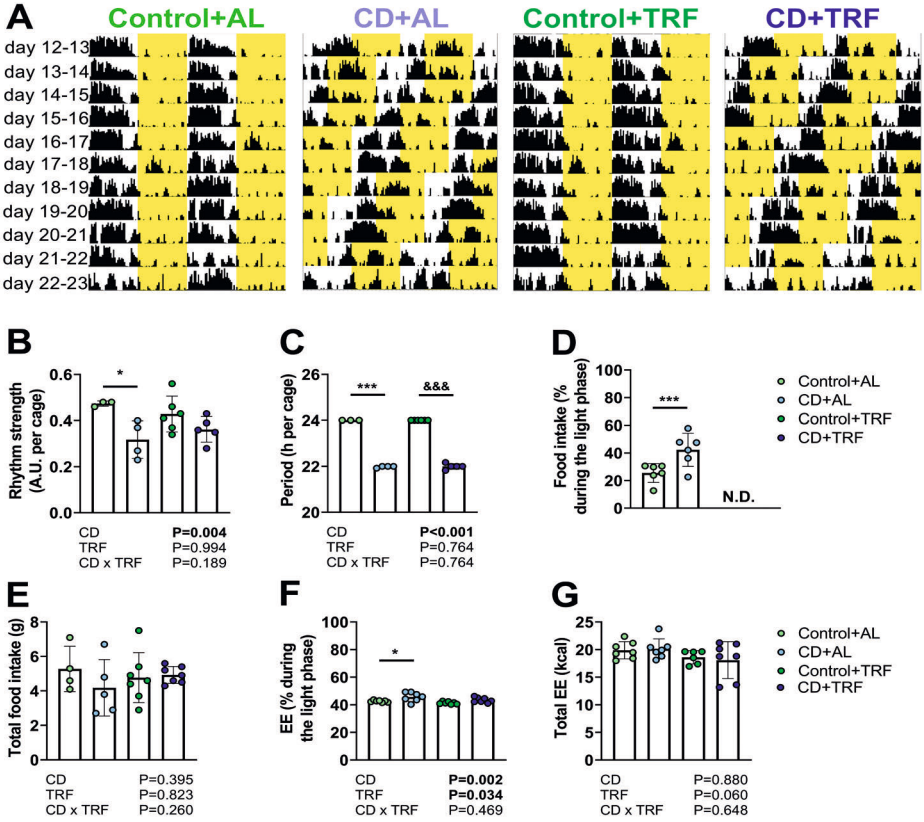

Figure 1. Rhythms of behavior and energy balance.

*APOE*3-Leiden.CETP mice were exposed to a 6-hour phase advancement every 3 days (circadian disturbance; CD) or regular 12:12 light-dark cycle (Control), while having either ad libitum food access (AL) or food access during the dark phase only (time-restricted feeding; TRF) for a total duration of 14 weeks. (**A**) Actograms of four consecutive shifts during the second cycle of phase shifts (days 12-23) of the study were constructed and periodogram analysis was used to calculate (**B**) rhythm strength (expressed as A.U., arbitrary unit) and (**C**) period (n=3-6 cages of 2-3 mice/group). During the sixth cycle of phase shifts, mice were housed in metabolic home-cages for continuous measurement of (**D, E**) food intake and (**F, G**) energy expenditure (EE), after which the percentage of each parameter during the light phase and the total levels were calculated (n=4-7 cages of 2-3 mice/group). Data are presented as means ± SD. * Control + AL vs. CD + AL; $^{\&}$Control + TRF vs. CD + TRF. * p<0.05; ***,$^{\&\&\&}$ p<0.001, according to unpaired t-test (D) or two-way ANOVA and following Tukey's multiple-comparison test (B-C, E-G).*

Time-restricted feeding attenuates atherosclerosis plaque size and macrophage content during circadian disturbance

Next, we evaluated atherosclerosis progression in the aortic root. While CD did not significantly increase atherosclerotic lesion area (Fig. 3a and b) or alter lesion severity, smooth muscle cell- or collagen-positive lesion area (Fig. 3a and c-f), the CD+AL group showed significantly increased macrophage-positive lesion area compared with Control+AL (Fig. 3a and g). In mice subjected to CD, TRF reduced atherosclerotic lesion

area (Fig. 3a and b) and tended to reduce lesion severity (Fig. 3c and d), while lowering smooth muscle cell-positive lesion area, but not collagen-positive lesion area (Fig. 3a and e-f). Strikingly, TRF fully prevented the elevation in macrophage content in lesions caused by CD (Fig. 3a and g). These findings suggest that TRF attenuates plaque progression during CD.

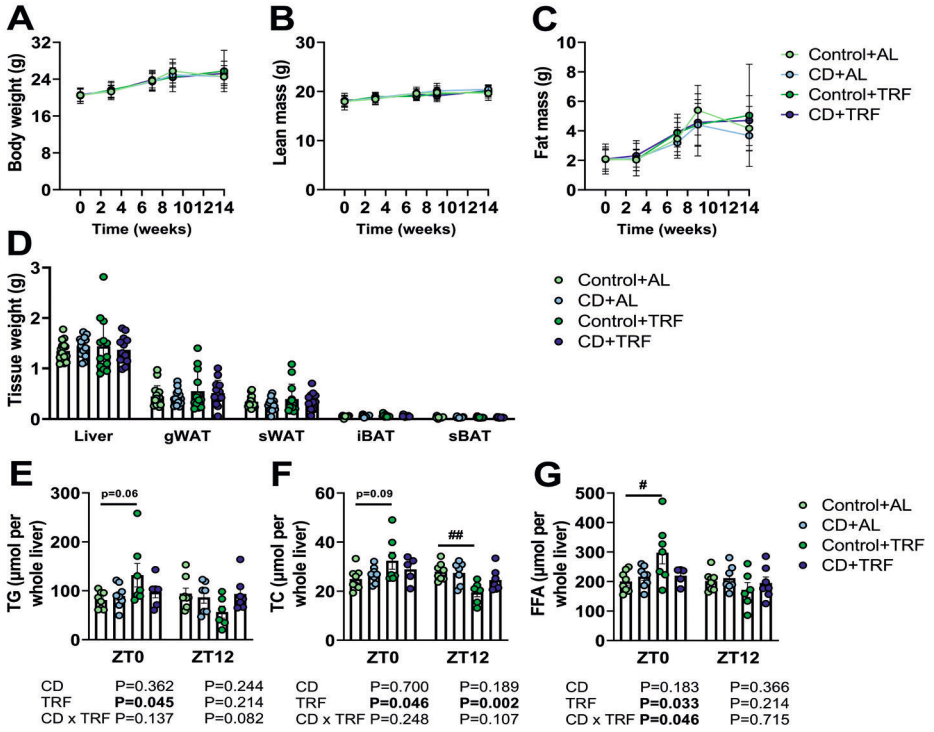

Figure 2. Body composition, tissue weights, and hepatic lipid content.

*APOE*3-Leiden.CETP mice were exposed to a 6-hour phase advancement every 3 days (circadian disturbance; CD) or regular 12:12 light-dark cycle (Control), while having either ad libitum food access (AL) or food access during the dark phase only (time-restricted feeding; TRF) for a total duration of 14 weeks. (**A**) Body weight, (**B**) lean mass, and (**C**) fat mass were monitored throughout the study. (**D**) Weight of liver, gonadal white adipose tissue (gWAT), subcutaneous WAT (sWAT), interscapular brown adipose tissue (iBAT) and subscapular BAT (sBAT) (n=13-16 mice/group) was assessed at the end of the study. Lipids were extracted from livers collected at Zeitgeber time (ZT)0 and 12 to measure (**E**) triglycerides (TG), (**F**) total cholesterol (TC), and (**G**) free fatty acids (FFA). Data are presented as means ± SD. #Control + AL vs. Control + TRF. # p<0.05; ## p<0.01, according to two-way ANOVA and following Tukey's multiple-comparison test.*

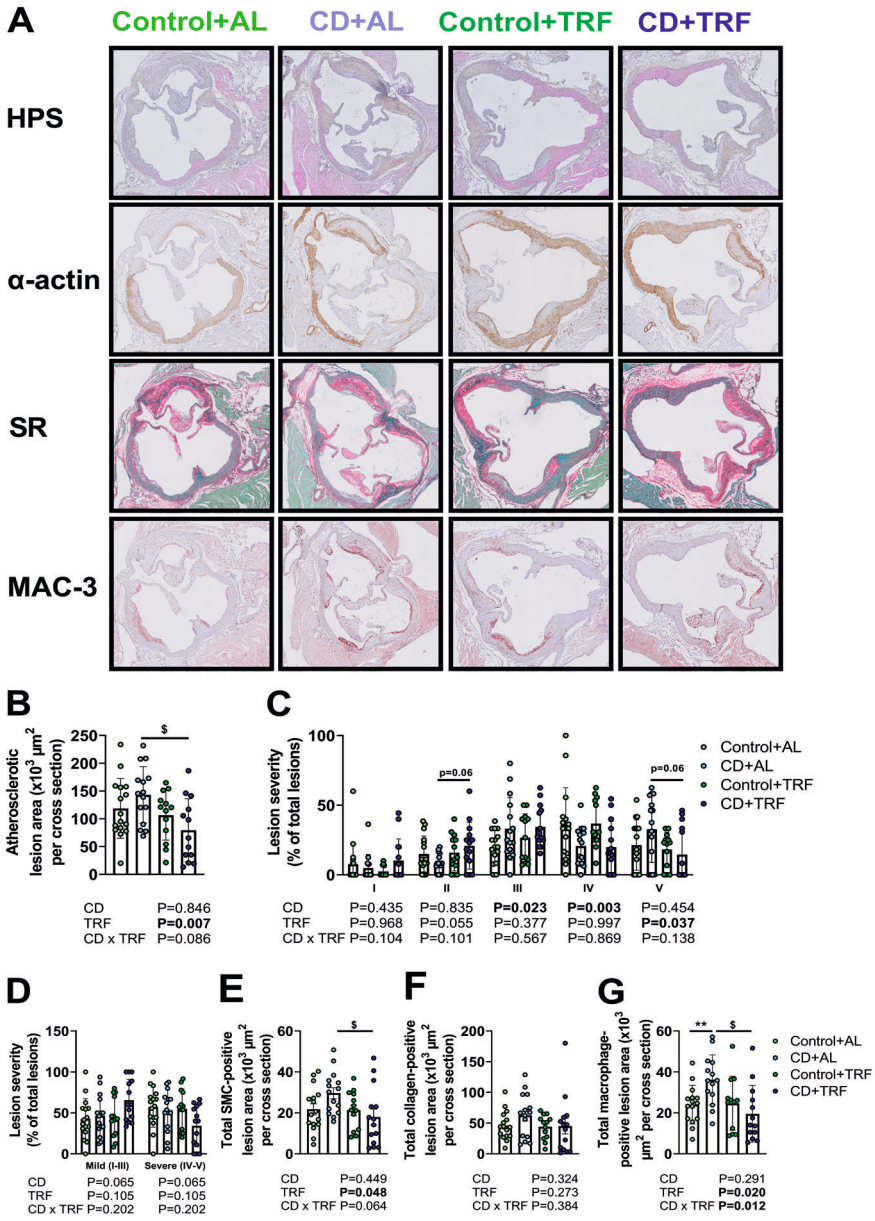

Figure 3. Atherosclerotic lesion size, severity, and composition.

*APOE*3-Leiden.CETP mice were exposed to a 6-hour phase advancement every 3 days (circadian disturbance; CD) or regular 12:12 light-dark cycle (Control), while having either ad libitum food access (AL) or food access during the dark phase only (time-restricted feeding; TRF) for a total duration of 14 weeks after which hearts were collected. Cross-sections of the aortic root area were stained with (**A**) hematoxylin-phloxine-saffron or with anti-α-actin antibody, Sirius Red (SR), or anti-MAC-3 antibody, and atherosclerotic lesion area was determined and expressed as a function of distance from the appearance of open aortic valves, (**B**) from which the mean atherosclerotic lesion area was calculated. Lesions were categorized according to lesion*

*severity, expressed as a percentage of total lesions, and shown (**C**) per lesion type (I-V) and (**D**) severity (mild; type I-III and severe; type IV-V). Using anti-α-actin antibody, SR, and anti-MAC-3 antibody-stained cross-sections, the (**E**) smooth muscle cell (SMC)-positive lesion area, (**F**) collagen-positive lesion area, and the (**G**) macrophage-positive lesion area was calculated (n=12-16 mice/group). Data are presented as means ± SD. $^{\$}$CD + AL vs. CD + TRF; * Control + AL vs. CD + AL. $^{\$}$ p<0.05; ** p<0.01, according to two-way ANOVA and following Tukey's multiple-comparison test.*

Time-restricted feeding increases circulating non-classical monocytes and attenuates the activated T cell profile caused by circadian disturbance

To obtain further insight in the mechanisms underlying the atherogenic effect of CD, and via which mechanisms TRF attenuates this risk, we first measured the relative abundance of circulating immune cell populations during the ninth cycle of phase shifts at ZT6 and ZT18 (12 and 24 hours after the last phase shift), as these time points correspond to the peak and trough levels of many immune cell populations in the blood, respectively.[9] We started with assessment of monocytes ($CD45^+$ $CD11b^+$), which play an essential role in atherosclerosis development, and can be distinguished as non-classical (Ly6Clow), intermediate (Ly6Cmed), and classical (Ly6Chi) monocytes. Non-classical monocytes are considered to be anti-inflammatory, whereas classical monocytes are considered to be pro-inflammatory and can adhere to activated endothelium and infiltrate the vessel wall after which they differentiate into macrophages.[21] With AL feeding, CD caused shifts in monocyte subtypes, by elevating the relative number of non-classical monocytes (CD effect at ZT18 by two-way ANOVA: P=0.047) (Fig. 4a), lowering intermediate monocytes (CD effect by two-way ANOVA: P<0.001 and P<0.001 for ZT6 and ZT18, respectively) (Fig. 4b), and elevating classical monocytes (CD effect at ZT6 by two-way ANOVA: P=0.001) (Fig. 4c). CD+TRF elevated non-classical monocytes when compared with Control+TRF and further reduced intermediate monocytes compared with CD+AL at ZT6 (CD-TRF interaction by two-way ANOVA: P=0.017), without preventing the elevation of classical monocytes caused by CD (Fig. 4a-c). These findings suggest that CD shifts the monocyte profile towards both anti-inflammatory non-classical and pro-inflammatory classical monocytes, and that TRF might be able to shift this balance towards more anti-inflammatory non-classical monocytes. Interestingly, eosinophils, which upon binding to the endothelium can promote leukocyte migration into the vessel wall,[22] were depleted by CD regardless of TRF (CD effect by two-way ANOVA: P<0.001 and P<0.001 at ZT6 and ZT18, respectively) (Fig. 4d).

Next, we looked at relative abundance of $CD4^+$ helper cells, which can be pro- or anti-atherogenic, depending on their polarization.[23] CD tended to increase the relative number of $CD4^+$ naïve cells ($CD44^-$ $CD62L^+$) and reduced effector $CD4^+$ cells ($CD62L^-$) regardless of TRF (CD effect by two-way ANOVA: P=0.024 and P<0.001 for ZT6 and ZT18, respectively) (Fig. 4e and f). CD+AL increased relative numbers of $CD4^+$ T central memory (Tcm) cells ($CD44^+$ $CD62L^+$) at ZT6 and ZT18 compared with Control+AL (Fig. 4g), which did not occur when mice were subjected to TRF during CD (CD-TRF interaction by two-way ANOVA: P=0.012 and P=0.020 for ZT6 and ZT18, respectively). The subset of

$CD4^+$ cells expressing C-X-C Motif Chemokine Receptor 3 (CXCR3), a chemokine receptor closely associated with the pro-atherogenic T helper 1 subset,[23] was unchanged by CD (Fig. 4h). In contrast to $CD4^+$ cells, the role of $CD8^+$ (cytotoxic T cells) in atherosclerosis is less-well understood and depending on their subset, can be considered both pro- and anti-atherogenic.[23] While CD did not alter $CD8^+$ naïve cells, CD reduced $CD8^+$ effector cells (CD effect by two-way ANOVA: P=0.004) and increased $CD8^+$ Tcm cells (CD effect by two-way ANOVA: P=0.030) (Fig. 4i-k). In line with $CD4^+$ Tcm cells (Fig. 4g), TRF prevented the increase in $CD8^+$ Tcm cells caused by CD (Fig. 4k). This might indicate that during the intervention, CD caused an activated T cell profile in the blood with AL feeding but not with TRF. Interestingly, CD and TRF alone (CD and TRF effect by two-way ANOVA: P=0.020 and P=0.024 for CD at ZT18 and TRF at ZT6, respectively), but not in combination (CD-TRF interaction by two-way ANOVA: P=0.039 and P=0.071 at ZT6 and ZT18, respectively), increased the relative abundance of $CXCR3^+$ cytotoxic T cells (Fig. 4l), which are considered to be pro-atherogenic.[23]

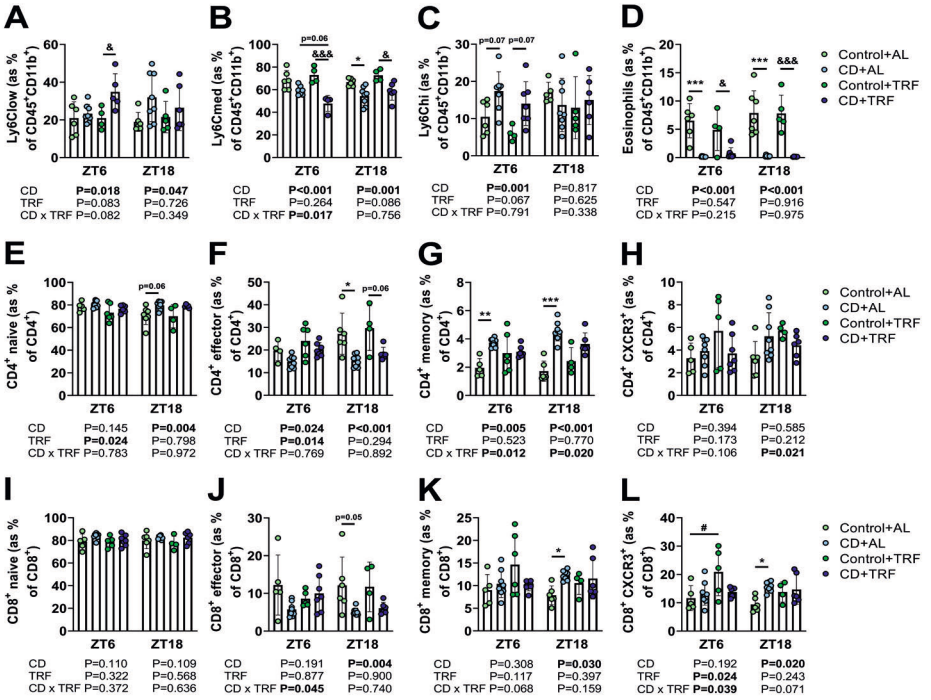

Figure 4. Circulating monocytes, eosinophils, and T cells.

*APOE*3-Leiden.CETP mice were exposed to a 6-hour phase advancement every 3 days (circadian disturbance; CD) or regular 12:12 light-dark cycle (Control), while having either ad libitum food access (AL) or food access during the dark phase only (time-restricted feeding; TRF) for a total duration of 14 weeks. During the ninth cycle of phase shifts, blood was collected to measure abundance of circulating (**A**) non-classical monocytes (Ly6Clow), (**B**) intermediate monocytes (Ly6Cmed), (**C**) classical monocytes (Ly6Chigh), (**D**) eosinophils, (**E**) cluster of differentiation (CD)4$^+$ naïve cells, (**F**) CD4$^+$ effector cells, (**G**) CD4$^+$ T central memory (Tcm) cells, (**H**) CD4$^+$ C-X-C Motif Chemokine Receptor 3 (CXCR3$^+$) cells, (**I**) CD8$^+$ naïve cells, (**J**) CD8$^+$ effector cells, (**K**) CD8$^+$ Tcm cells, and (**L**) CD8$^+$ CXCR3$^+$ cells using flow cytometry (n=4-8 mice/group/time point). Data are presented as means ± SD. $^{\#}$Control + AL vs. Control + TRF; * Control + AL vs. CD + AL; $^{\&}$Control + TRF vs. CD + TRF. $^{\#,*,\&}$ p<0.05; ** p<0.01; $^{***,\&\&\&}$ p<0.001, according to two-way ANOVA and following Tukey's multiple-comparison test.*

Time-restricted feeding reduces plasma total cholesterol levels during circadian disturbance

We next focused on plasma lipids that are tightly linked to atherosclerosis development,[24] and show large diurnal variation. Plasma lipid levels were assessed during the third cycle of phase shifts at ZT0, ZT6, ZT12, and ZT18 (24, 30, 12, and 18 hours after the last phase shift for ZT0, ZT6, ZT12, and ZT18, respectively). CD attenuated diurnal rhythmicity of plasma TG and TC levels (time-CD interaction by three-way ANOVA: P<0.001 and P=0.083 for TG and TC, respectively) (Fig. 5a and c). While TRF by itself slightly elevated total plasma TG levels (TRF effect by two-way ANOVA: P=0.009) (Fig. 5b), TRF prevented the attenuations in diurnal plasma TG and TC levels caused by CD (time-CD-TRF interaction by three-way ANOVA: P<0.001 and P=0.085 for TG and TC,

respectively) (Fig. 5a and c) and lowered total plasma TC levels during CD (Fig. 5c and d). We next performed an oral lipid tolerance test at the time point when TG levels were elevated in the CD groups (i.e. ZT12, 12 hours after the last phase shift) to find CD delayed postprandial TG excursions, regardless of TRF (CD effect by two-way ANOVA: P=0.004) (Fig. 5e and f). Notably, CD increased TC exposure throughout the study (CD effect by two-way ANOVA: P=0.029) and TRF reduced TC exposure in mice subjected to CD (Fig. 5g and h). Importantly, TC exposure throughout the study correlated with atherosclerotic lesion area and with the macrophage-positive lesion area (Fig. 5i and j). These data suggest that TRF counteracts atherosclerosis development by attenuating hypercholesterolemia during CD.

Next, we investigated if altered lipid handling by peripheral organs could explain the elevated plasma TG levels and postprandial TG excursions at ZT12 caused by CD and/or the reduced plasma TC levels upon TRF during CD. We therefore assessed plasma clearance and tissue uptake of glycerol tri[^{3}H]oleate and [^{14}C]cholesteryl oleate from intravenously-injected TG-rich lipoprotein-like particles at the study endpoint at ZT0 and ZT12 (24 and 12 hours after the last phase shift for ZT0 and ZT12, respectively). In line with delayed postprandial TG excursions (Fig. 5e and f), CD delayed the plasma decay of ^{3}H-derived activity at ZT12 regardless of TRF (CD effect by two-way ANOVA: P<0.001) (Fig. 6a-c), an effect explained by reduced uptake of [^{3}H]oleate by WAT and BAT (CD effect at ZT12 by two-way ANOVA: P=0.009, P=0.058, P<0.001, and P=0.004 for gonadal (g)WAT, subcutaneous (s)WAT, interscapular (i)BAT, and subscapular (s)BAT, respectively) (Fig. 6g-j). Plasma decay of ^{14}C-derived activity was unchanged with CD (Fig. 6d-f) and hepatic uptake of [^{14}C]cholesteryl oleate was reduced at ZT0 regardless of TRF (CD effect by two-way ANOVA: P=0.020) (Fig. 6k), indicating that TRF does not reduce plasma TC levels during CD by enhancing TRL-remnant uptake by the liver.

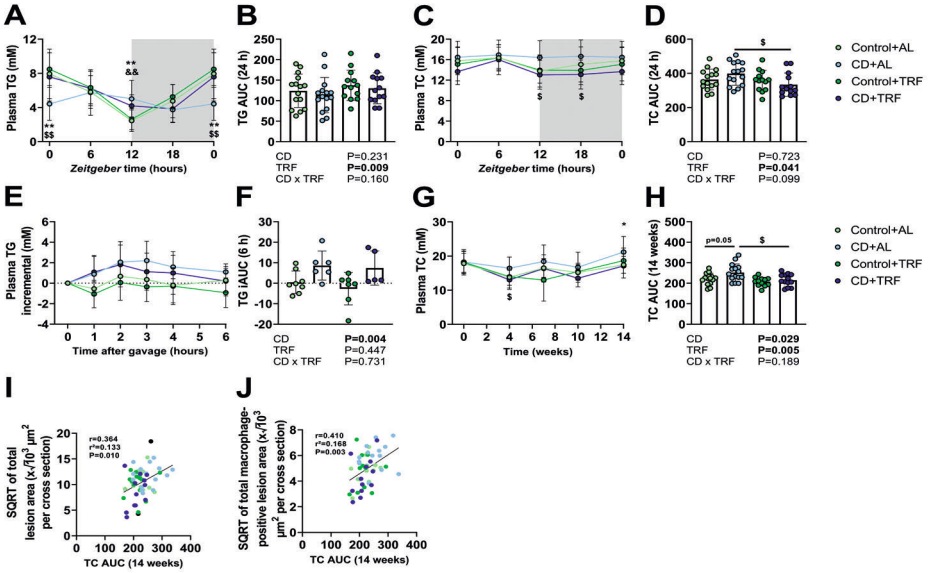

Figure 5. Diurnal and postprandial plasma lipid levels.

*APOE*3-Leiden.CETP mice were exposed to a 6-hour phase advancement every 3 days (circadian disturbance; CD) or regular 12:12 light-dark cycle (Control), while having either ad libitum food access (AL) or food access during the dark phase only (time-restricted feeding; TRF) for a total duration of 14 weeks. During the third cycle of phase shifts, plasma was collected at Zeitgeber time (ZT)0, 6, 12, and 18 to measure (**A**) triglycerides (TG) (**B**) from which the area under the curve (AUC) was calculated, and (**C**) total cholesterol (TC) (**D**) from which the AUC was calculated (n=13-15 mice/group). ZT0 is double-plotted. During the seventh cycle of phase shifts at ZT12, mice received an oral olive oil bolus to measure postprandial (**E**) plasma TG levels (**F**) from which the AUC was calculated (n=5-8 mice/group). (**G**) Plasma TC levels were monitored throughout the study (**H**) from which the AUC was calculated (n=12-15 mice/group). The total cholesterol exposure throughout the study (TC AUC) was plotted against the square root of the (**I**) total lesion area and (**J**) total MAC-3 positive lesion area from which B and Pearson correlation coefficients were determined. Data are presented as means ± SD. $CD + AL vs. CD + TRF; * Control + AL vs. CD + AL; &Control + TRF vs. CD + TRF. $ p<0.05; &&,** p<0.01, according to two-way ANOVA and following Tukey's multiple-comparison test.*

Since the liver is the primary organ of cholesterol production and secretion, we next investigated hepatic expression of genes involved in cholesterol metabolism besides those involved in the cellular clock. CD profoundly altered clock gene expression at ZT12, suggestive of shifts in hepatic rhythms (Fig. 7a-c). The shift in *Per2* expression at ZT0 tended to be attenuated by TRF (CD-TRF interaction with two-way ANOVA: P=0.052). Both CD and TRF did not markedly alter the expression of microsomal triglyceride transfer protein (*Mttp*) and apolipoprotein B (*Apob*), genes encoding proteins that are involved in very-low-density lipoprotein (VLDL) production, cholesterol 7 alpha-hydroxylase (*Cyp7a1*) that regulates bile acid synthesis, or ATP-binding cassette sub-family G member 5 (*Abcg5*), a regulator of sterol secretion towards the bile (Fig. 7d-g). Interestingly, TRF did attenuate sterol regulatory element-binding protein 2 (*Srebp2*) expression at ZT12 (CD-TRF interaction by two-way ANOVA: P=0.019) (Fig. 7h), and the CD+TRF group showed a pronounced reduction in *Hmgcr* expression at both ZT0 and ZT12 compared with the CD+AL group, albeit non-significantly at ZT0, indicating reduced cholesterol synthesis (Fig. 7i).

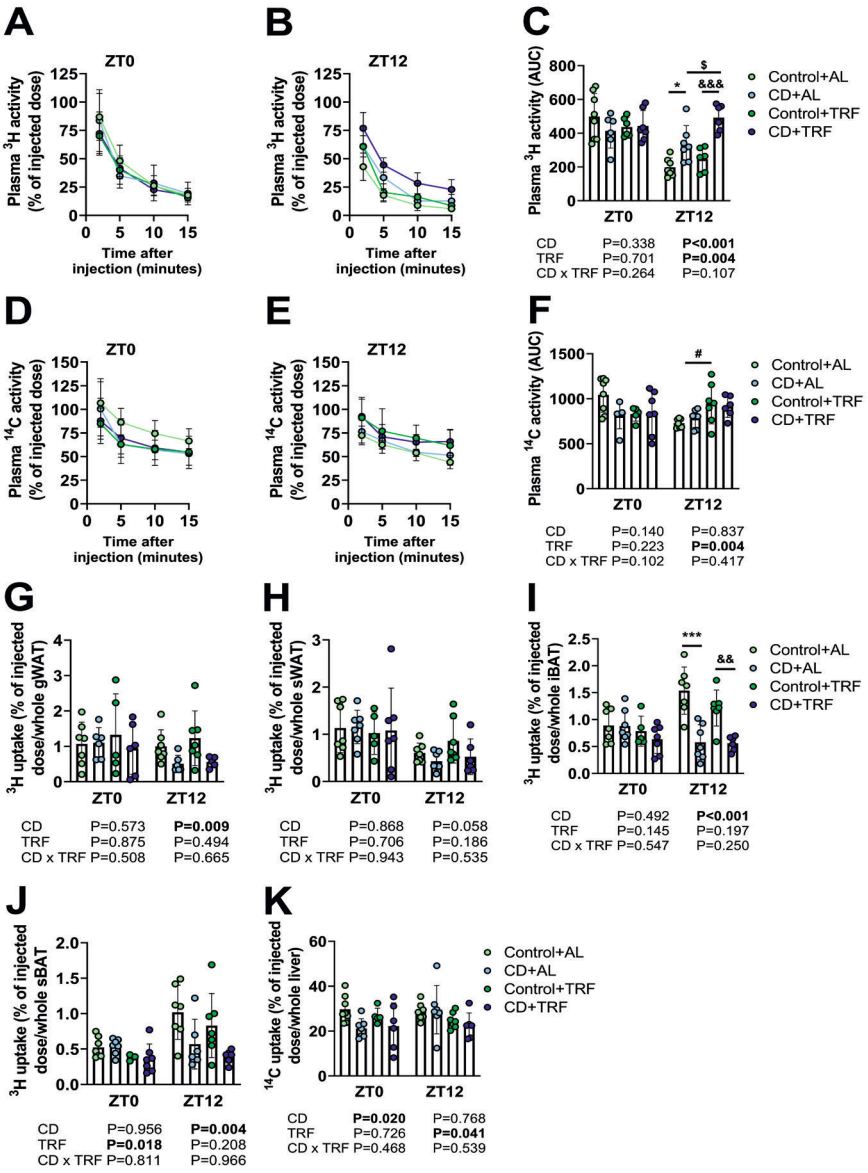

Figure 6. Diurnal variation in clearance and uptake of triglyceride-rich lipoproteins (TRLs) and TRL-remnants.

*APOE*3-Leiden.CETP mice were exposed to a 6-hour phase advancement every 3 days (circadian disturbance; CD) or regular 12:12 light-dark cycle (Control), while having either ad libitum food access (AL) or food access during the dark phase only (time-restricted feeding; TRF) for a total duration of 14 weeks. After 14 weeks, mice were injected with TRL-like particles double-labeled with glycerol tri[^{3}H]oleate and [^{14}C]cholesteryl oleate at ZT0 and 12 to assess plasma decay of (**A, B, C**) [^{3}H]oleate (n=5-8 mice/group/time point) and (**D, E, F**) [^{14}C]cholesteryl oleate and [^{3}H]oleate uptake by (**G**) gonadal white adipose tissue (gWAT), (**H**) subcutaneous WAT (sWAT), (**I**) interscapular brown adipose tissue (iBAT), (**J**) and subscapular BAT (sBAT), and (**K**) [^{14}C]cholesteryl oleate uptake by the liver (n=5-7 mice/group/time point). Data are presented as means ± SD. $^{\$}$CD + AL vs. CD + TRF; * Control + AL vs. CD + AL; $^{\&}$Control + TRF vs. CD + TRF. $^{\$,*,\#}$ p<0.05; $^{\&\&}$ p<0.01; $^{***,\&\&\&}$ p<0.001, according to two-way ANOVA and following Tukey's multiple-comparison test.*

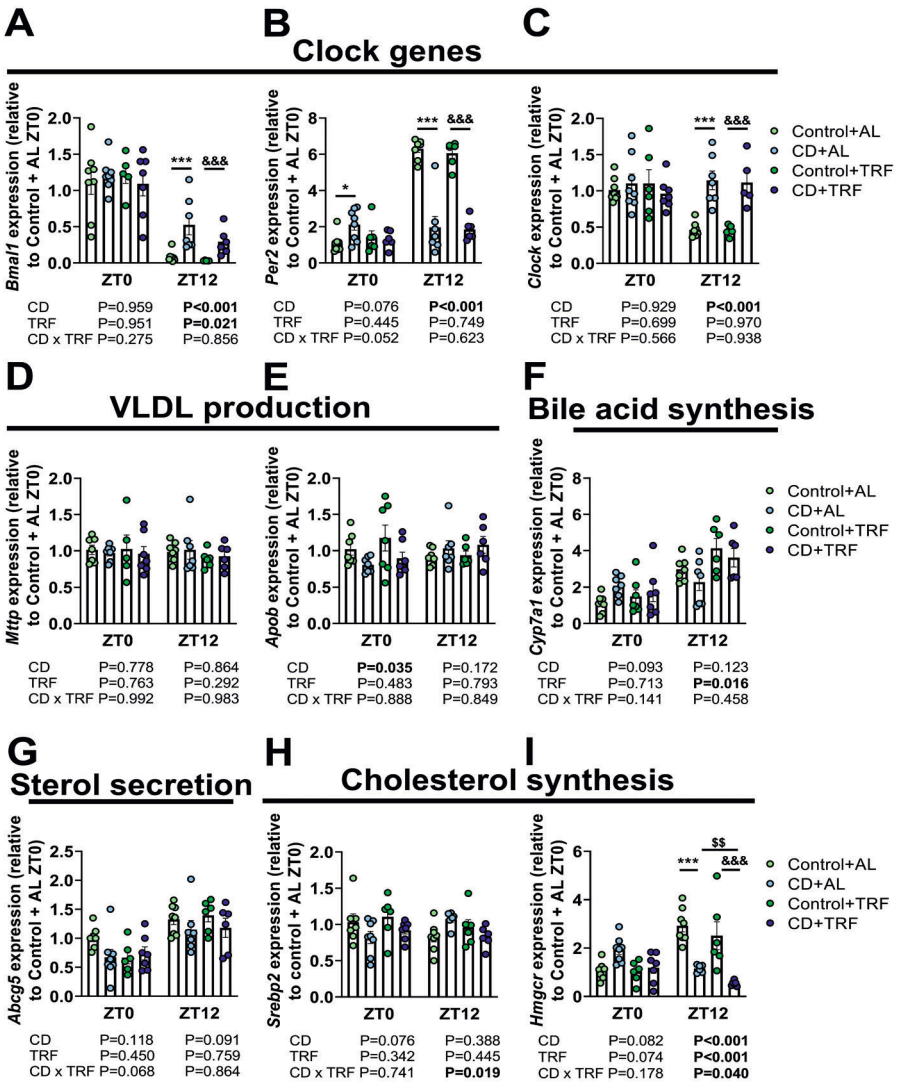

Figure 7. Hepatic expression of genes involved in the core clock machinery and cholesterol metabolism.

*APOE*3-Leiden.CETP mice were exposed to a 6-hour phase advancement every 3 days (circadian disturbance; CD) or regular 12:12 light-dark cycle (Control), while having either ad libitum food access (AL) or food access during the dark phase only (time-restricted feeding; TRF) for a total duration of 14 weeks. Hepatic gene expression of (**A**) brain and muscle Arnt-like protein-1 (Bmal1), (**B**) period 2 (Per2), (**C**) circadian locomotor output cycles kaput (Clock), (**D**) microsomal triglyceride transfer protein (Mttp), (**E**) apolipoprotein B (Apob), (**F**) cholesterol 7 alpha-hydroxylase (Cyp7a1), (**G**) ATP-binding cassette sub-family G member 5 (Abcg5), (**H**) sterol regulatory element-binding protein 2 (Srebp2), and (**I**) 3-hydroxy-3-methyl-glutaryl-coenzyme A reductase (Hmgcr) at Zeitgeber time (ZT) 0 and 12, as determined by quantitative polymerase chain reaction, normalized to glyceraldehyde-3-phosphate dehydrogenase (Gapdh) and shown relative to the expression in control AL ZT0 (n=5-8 mice/group/time point). Data are presented as means ± SD. $^{\$}$CD + AL vs. CD + TRF; * Control + AL vs. CD + AL; $^{\&}$Control + TRF vs. CD + TRF. * p<0.05; $^{\$\$}$ p<0.01; ***$^{\&\&\&}$ p<0.001, according to two-way ANOVA and following Tukey's multiple-comparison test.*

Discussion

CD, which frequently occurs during shift work, has been associated with increased asCVD risk in humans, but evidence for the effectiveness of prevention strategies are lacking. Here, we assessed if TRF is a viable strategy to prevent elevated asCVD risk caused by CD. To this end, CD was modeled in APOE*3-Leiden.CETP mice through repeated shifts in the light-dark cycles, which resulted in a non-significant elevation in atherosclerotic lesion size and significantly increased macrophage content within the lesions. We demonstrate that restricting food intake to the dark phase completely prevents the increase in atherosclerotic lesion area and macrophage content caused by CD.

Inflammatory processes involved in atherogenesis are under control of the circadian clock, including the abundance of circulating immune cells in both mice and humans.[9,25] Disturbance of circadian rhythms by genetic deletion of clock genes in mice results in a pro-inflammatory immune cell profile as well as higher macrophage infiltration in atherosclerotic lesions.[26-28] In our study, we observed that CD modulates the immune system by inducing shifts in monocyte profile, depleting eosinophil levels, and causing an activated T cell profile in blood. During CD, TRF further increased anti-inflammatory non-classical monocytes and appeared to prevent the activated T cell profile in blood. In addition, we observed that CD elevated (postprandial) TG levels, coinciding with reduced lipid uptake by WAT and BAT at the onset of the dark phase. Accordingly, plasma lipid levels and lipid uptake by BAT follow a pronounced diurnal rhythm,[24,29] and CD was previously shown to attenuate rhythmic lipid uptake by BAT and elevate plasma lipid levels.[30,31] This suggests that restoring diurnal rhythms in adipose tissue is a potential therapeutic strategy to prevent elevations in plasma TGs caused by CD. These observations in mice are very comparable to what has previously been reported for humans, as levels of circulating immune cells and lipids also follow a diurnal rhythm, and shift work has been associated with systemic inflammation and dyslipidemia.[24,32-37]

In our study, TRF did not prevent the increase in pro-inflammatory monocytes or the elevated (postprandial) plasma TG levels caused by CD. Of all tissues, the liver appears to be most responsive to altered feeding patterns.[38] In line with this notion, TRF lowered markers of hepatic cholesterol synthesis during CD, which possibly underlies the attenuation of hypercholesterolemia. Avoiding food intake during the inactive phase by applying TRF may thereby prevent disturbances in hepatic lipid metabolism during CD.

Surprisingly, TRF without the context of CD did not markedly improve asCVD risk factors or atherosclerosis progression in our study. The finding that TRF alone did not improve asCVD risk factors suggests that TRF is only beneficial in mice when diurnal eating patterns are disturbed by e.g. CD or diet-induced obesity.[39,40] In humans, TRE has shown to improve cardiometabolic health, but the question remains to what extent the effects of TRE surpass those of calorie reduction.[41] We now show that independent of total food

intake, TRF attenuates atherosclerosis development in the context of CD. We therefore propose that TRE could be a potential strategy for the primary prevention of elevated asCVD risk in shift workers, which warrants future study in humans. In this respect, it is reassuring that a recent pioneering study demonstrated that TRE is safe and feasible in a population of shift workers.[42]

In addition to timed food intake, other *Zeitgebers* could be exploited to mitigate elevated asCVD risk during shift work. For example, physical activity acts as a *Zeitgeber*, as timed exercise can shift behavioral rhythms in mice by modulating the molecular muscle clock.[43,44] Timed exercise alone or in combination with TRE might therefore be a promising strategy to minimize adverse effects of CD on cardiometabolic health. Optimization of timed exercise and eating interventions likely requires personalized adjustments, as high inter-individual variability exists in the circadian system and shift work tolerance, i.e., the ability to adapt to shift work without adverse consequences such as digestive troubles, persisting fatigue, and sleep alteration. This variation in circadian rhythms and shift work tolerance is caused by factors such as genetics, age, sex, and chronotype,[45] as well as the time window at which the night shift takes place, whether the shifts are permanent or rotating, the total number of consecutive shifts, and the work place conditions including lighting conditions.[46] Similarly, responsiveness to circadian interventions may be variable as one study demonstrated that circadian phase shifts caused by timed exercise vary with chronotype.[47] Future research should therefore characterize inter-individual differences in the phase-shifting response to timed eating and exercise, which could contribute to development of personalized interventions for primary disease prevention in shift working populations.

Acknowledgements

We thank Johanna H. Meijer for providing us with the Clocklab software.

Funding

M.S. is supported by the Novo Nordisk Foundation (NNF18OC0032394). L.A.B. is supported by a Amsterdam Cardiovascular Science Post Doctoral Grant. P.C.N.R. is supported by the Netherlands Cardiovascular Research Initiative: an initiative with support of the Dutch Heart Foundation (CVON-GENIUS-II). S.K. is supported by the Dutch Heart Foundation (2017T016). L.W.M.K and M.E.T.D were supported by a grant from the Netherlands Ministry of Social Affairs and Employment (KV 110016).

References

1. (WHO) WHO. Factsheet 'Cardiovascular diseases' 2021. https://www.who.int/news-room/fact-sheets/detail/cardiovascular-diseases-(cvds) (accessed 05-10 2022).
2. Libby P. The changing landscape of atherosclerosis. *Nature* 2021; **592**(7855): 524-33.
3. Sun M, Feng W, Wang F, Li P, Li Z, Li M, et al. Meta-analysis on shift work and risks of specific obesity types. *Obesity reviews* 2018; **19**(1): 28-40.
4. Esquirol Y, Perret B, Ruidavets JB, Marquie JC, Dienne E, Niezborala M, et al. Shift work and cardiovascular risk factors: new knowledge from the past decade. *Archives of cardiovascular diseases* 2011; **104**(12): 636-68.
5. McHill A, Wright Jr K. Role of sleep and circadian disruption on energy expenditure and in metabolic predisposition to human obesity and metabolic disease. *Obesity reviews* 2017; **18**: 15-24.
6. Karlsson B, Knutsson A, Lindahl B. Is there an association between shift work and having a metabolic syndrome? Results from a population based study of 27 485 people. *Occupational and environmental medicine* 2001; **58**(11): 747-52.
7. Scheer FA, Hilton MF, Mantzoros CS, Shea SA. Adverse metabolic and cardiovascular consequences of circadian misalignment. *Proceedings of the National Academy of Sciences* 2009; **106**(11): 4453-8.
8. Opperhuizen A-L, van Kerkhof LW, Proper KI, Rodenburg W, Kalsbeek A. Rodent models to study the metabolic effects of shiftwork in humans. *Frontiers in pharmacology* 2015; **6**: 50.
9. Schilperoort M, van den Berg R, Bosmans LA, van Os BW, Dollé ME, Smits NA, et al. Disruption of circadian rhythm by alternating light-dark cycles aggravates atherosclerosis development in APOE* 3-Leiden. CETP mice. *Journal of pineal research* 2020; **68**(1): e12614.
10. Zadelaar ASM, Boesten LS, Jukema JW, van Vlijmen BJ, Kooistra T, Emeis JJ, et al. Dual PPARα/γ agonist tesaglitazar reduces atherosclerosis in insulin-resistant and hypercholesterolemic ApoE* 3Leiden mice. *Arteriosclerosis, thrombosis, and vascular biology* 2006; **26**(11): 2560-6.
11. Westerterp M, van der Hoogt CC, de Haan W, Offerman EH, Dallinga-Thie GM, Jukema JW, et al. Cholesteryl ester transfer protein decreases high-density lipoprotein and severely aggravates atherosclerosis in APOE* 3-Leiden mice. *Arteriosclerosis, thrombosis, and vascular biology* 2006; **26**(11): 2552-9.
12. Regmi P, Heilbronn LK. Time-restricted eating: benefits, mechanisms, and challenges in translation. *Iscience* 2020; **23**(6): 101161.
13. He M, Wang J, Liang Q, Li M, Guo H, Wang Y, et al. Time-restricted eating with or without low-carbohydrate diet reduces visceral fat and improves metabolic syndrome: A randomized trial. *Cell Reports Medicine* 2022; **3**(10): 100777.
14. Bass J, Takahashi JS. Circadian integration of metabolism and energetics. *Science* 2010; **330**(6009): 1349-54.
15. Schilperoort M, van den Berg R, Dollé ME, van Oostrom C, Wagner K, Tambyrajah LL, et al. Time-restricted feeding improves adaptation to chronically alternating light-dark cycles. *Scientific reports* 2019; **9**(1): 1-12.
16. Van Vlijmen B, van't Hof HB, Mol M, van der Boom H, van der Zee A, Frants RR, et al. Modulation of very low density lipoprotein production and clearance contributes to age- and gender-dependent hyperlipoproteinemia in apolipoprotein E3-Leiden transgenic mice. *The Journal of clinical investigation* 1996; **97**(5): 1184-92.
17. van Eenige R, Verhave PS, Koemans PJ, Tiebosch IA, Rensen PC, Kooijman S. RandoMice, a novel, user-friendly randomization tool in animal research. *Plos one* 2020; **15**(8): e0237096.

18. Jenni OG, Deboer T, Achermann P. Development of the 24-h rest-activity pattern in human infants. *Infant behavior and development* 2006; **29**(2): 143-52.

19. Stenvers DJ, van Dorp R, Foppen E, Mendoza J, Opperhuizen A-L, Fliers E, et al. Dim light at night disturbs the daily sleep-wake cycle in the rat. *Scientific reports* 2016; **6**(1): 1-12.

20. Ying Z, Boon MR, Coskun T, Kooijman S, Rensen PC. A simplified procedure to trace triglyceride-rich lipoprotein metabolism in vivo. *Physiological Reports* 2021; **9**(8): e14820.

21. Hilgendorf I, Swirski FK, Robbins CS. Monocyte fate in atherosclerosis. *Arteriosclerosis, thrombosis, and vascular biology* 2015; **35**(2): 272-9.

22. Mackman N. Eosinophils, atherosclerosis, and thrombosis. *Blood, The Journal of the American Society of Hematology* 2019; **134**(21): 1781-2.

23. Saigusa R, Winkels H, Ley K. T cell subsets and functions in atherosclerosis. *Nature Reviews Cardiology* 2020; **17**(7): 387-401.

24. van den Berg R, Kooijman S, Noordam R, Ramkisoensing A, Abreu-Vieira G, Tambyrajah LL, et al. A diurnal rhythm in brown adipose tissue causes rapid clearance and combustion of plasma lipids at wakening. *Cell reports* 2018; **22**(13): 3521-33.

25. Lange T, Dimitrov S, Born J. Effects of sleep and circadian rhythm on the human immune system. *Annals of the New York Academy of Sciences* 2010; **1193**(1): 48-59.

26. Gibbs JE, Blaikley J, Beesley S, Matthews L, Simpson KD, Boyce SH, et al. The nuclear receptor REV-ERBα mediates circadian regulation of innate immunity through selective regulation of inflammatory cytokines. *Proceedings of the National Academy of Sciences* 2012; **109**(2): 582-7.

27. Huo M, Huang Y, Qu D, Zhang H, Wong WT, Chawla A, et al. Myeloid Bmal1 deletion increases monocyte recruitment and worsens atherosclerosis. *The FASEB Journal* 2017; **31**(3): 1097-106.

28. Sato S, Sakurai T, Ogasawara J, Takahashi M, Izawa T, Imaizumi K, et al. A circadian clock gene, Rev-erbα, modulates the inflammatory function of macrophages through the negative regulation of Ccl2 expression. *The Journal of Immunology* 2014; **192**(1): 407-17.

29. van Eenige R, het Panhuis WI, Schönke M, Jouffe C, Devilee TH, Siebeler R, et al. Angiopoietin-like 4 governs diurnal lipoprotein lipase activity in brown adipose tissue. *Molecular Metabolism* 2022; **60**: 101497.

30. Kooijman S, van den Berg R, Ramkisoensing A, Boon MR, Kuipers EN, Loef M, et al. Prolonged daily light exposure increases body fat mass through attenuation of brown adipose tissue activity. *Proceedings of the National Academy of Sciences* 2015; **112**(21): 6748-53.

31. Chalfant JM, Howatt DA, Tannock LR, Daugherty A, Pendergast JS. Circadian disruption with constant light exposure exacerbates atherosclerosis in male ApolipoproteinE-deficient mice. *Scientific reports* 2020; **10**(1): 1-11.

32. Yuan RK, Zitting KM, Wang W, Buxton OM, Williams JS, Duffy JF, et al. Fasting blood triglycerides vary with circadian phase in both young and older people. *Physiological reports* 2020; **8**(11): e14453.

33. Dutheil F, Baker JS, Mermillod M, De Cesare M, Vidal A, Moustafa F, et al. Shift work, and particularly permanent night shifts, promote dyslipidaemia: A systematic review and meta-analysis. *Atherosclerosis* 2020; **313**: 156-69.

34. Matre D, Christensen J, Mork P, Ferreira P, Sand T, Nilsen K. Shift work, inflammation and musculoskeletal pain—The HUNT Study. *Occupational Medicine* 2021; **71**(9): 422-7.

35. Cuesta M, Boudreau P, Dubeau-Laramée G, Cermakian N, Boivin DB. Simulated night shift disrupts circadian rhythms of immune functions in humans. *The Journal of Immunology* 2016; **196**(6): 2466-75.

36. Sookoian S, Gemma C, Fernandez Gianotti T, Burgueno A, Alvarez A, Gonzalez C, et al. Effects of rotating shift work on biomarkers of metabolic syndrome and inflammation. *Journal of internal medicine* 2007; **261**(3): 285-92.

37. Morris CJ, Purvis TE, Hu K, Scheer FA. Circadian misalignment increases cardiovascular disease risk factors in humans. *Proceedings of the National Academy of Sciences* 2016; **113**(10): E1402-E11.

38. Panda S. Circadian physiology of metabolism. *Science* 2016; **354**(6315): 1008-15.

39. Chaix A, Lin T, Le HD, Chang MW, Panda S. Time-restricted feeding prevents obesity and metabolic syndrome in mice lacking a circadian clock. *Cell metabolism* 2019; **29**(2): 303-19. e4.

40. Brown MR, Sen SK, Mazzone A, Her TK, Xiong Y, Lee J-H, et al. Time-restricted feeding prevents deleterious metabolic effects of circadian disruption through epigenetic control of β cell function. *Science Advances* 2021; **7**(51): eabg6856.

41. Rynders CA, Thomas EA, Zaman A, Pan Z, Catenacci VA, Melanson EL. Effectiveness of intermittent fasting and time-restricted feeding compared to continuous energy restriction for weight loss. *Nutrients* 2019; **11**(10): 2442.

42. Manoogian EN, Zadourian A, Lo HC, Gutierrez NR, Shoghi A, Rosander A, et al. Feasibility of time-restricted eating and impacts on cardiometabolic health in 24-h shift workers: The Healthy Heroes randomized control trial. *Cell Metabolism* 2022; **34**(10): 1442-56. e7.

43. Wolff G, Esser KA. Scheduled exercise phase shifts the circadian clock in skeletal muscle. *Medicine and science in sports and exercise* 2012; **44**(9): 1663.

44. Yamanaka Y, Honma S, Honma Ki. Scheduled exposures to a novel environment with a running-wheel differentially accelerate re-entrainment of mice peripheral clocks to new light–dark cycles. *Genes to Cells* 2008; **13**(5): 497-507.

45. Saksvik IB, Bjorvatn B, Hetland H, Sandal GM, Pallesen S. Individual differences in tolerance to shift work–a systematic review. *Sleep medicine reviews* 2011; **15**(4): 221-35.

46. Kervezee L, Kosmadopoulos A, Boivin DB. Metabolic and cardiovascular consequences of shift work: The role of circadian disruption and sleep disturbances. *European Journal of Neuroscience* 2020; **51**(1): 396-412.

47. Thomas JM, Kern PA, Bush HM, McQuerry KJ, Black WS, Clasey JL, et al. Circadian rhythm phase shifts caused by timed exercise vary with chronotype. *JCI insight* 2020; **5**(3).